Gluon saturation and net-proton spectra in relativistic nucleus-nucleus collisions*

WANG Hong-Min(王宏民)[1;1)] HOU Zhao-Yu(侯召宇)[2]
WANG Xiu-Ting(王秀庭)[1] SUN Xian-Jing(孙献静)[3]

[1] Physics Department, Academy of Armored Forces Engineering of PLA, Beijing 100072, China
[2] Physics Graduate School, Shijiazhuang Railway Institute, Shijiazhuang 050043, China
[3] Institute of High Energy Physics, Chinese Academy of Sciences, Beijing 100049, China

Abstract: By means of the AKK08 fragmentation function, the net-proton transverse momentum ($p_{\rm T}$) spectra in A+A collisions are studied with two phenomenological models based on the Color Glass Condensate formalism. After a χ^2 analysis of the experimental data from BRAHMS, the normalization constant C is extracted at RHIC energies of $\sqrt{s_{\rm NN}}$ =62.4 and 200 GeV, and the theoretical results of the net-proton $p_{\rm T}$ spectra at selected rapidities are also given. It is shown that the theoretical results are in good agreement with the experimental data. Finally, assuming the constant C should have an exponent dependence of $\sqrt{s_{\rm NN}}$, we also predict the theoretical results of net-proton $p_{\rm T}$ spectra at LHC energies of $\sqrt{s_{\rm NN}}=2.76$, 3.94, and 5.52 TeV.

Key words: relativistic heavy-ion collisions, gluon saturation, net-proton spectra

PACS: 24.85.+p, 12.38.Cy, 25.75.-q **DOI:** 10.1088/1674-1137/35/3/008

1 Introduction

The investigation of gluon saturation has been an important and interesting subject of particle-physics on both the experimental and theoretical sides for many years. The observation of this phenomenon will access a new regime of Quantum Chromodynamics (QCD): the Color Glass Condensate (CGC) [1]. In this regime, where gluon recombination starts to counteract the effect of increasing gluon splitting, the gluon distribution function is expected to saturate and high-density gluons form a coherent state. Some evidence for gluon saturation in protons has been observed in e−p deep inelastic scattering (DIS) at HERA [2]. Related observations of the suppression of high $p_{\rm T}$ hadron yields have also been performed at the Relativistic Heavy-Ion Collider (RHIC) in deuteron-gold (d+Au) collisions [3]. The observed suppression shows that the modification factor is suppressed at forward rapidities, which are in qualitative agreement with the parton saturation predictions [4–6]. The gluon saturation can be further tested at the forthcoming Pb+Pb experiments at the Large Hadron Collider (LHC). In the present investigation, the transverse momentum spectra of net baryons will be used as a testing ground for saturation physics.

As a probe of QCD-matter at high parton density, net baryon production in relativistic heavy-ion collisions is an ideal tool to study the saturation regime. As the baryon number is conserved, we assume that the net-baryon number is essentially transported by valence quarks in one nucleus scatter in the other nucleus by exchanging soft gluons. Since the valence quark parton distribution is well known, this picture provides a clean proof of the unintegrated gluon distribution (UDG), $\varphi(x,q_{\rm T})$, in the saturation regime. In this paper, the unintegrated gluon distribution in the saturation regime will be studied with two distinct phenomenological models: the DHJ (Dumitru Hayashigaki and Jalilian-Marian) model [7] and the BUW (Boer Utermann and Wessels) model [8]. These two models for the UDG of the gold nucleus are inspired by approximate solutions of the Balitsky-Kovchegov (BK) equation [9, 10], in which both linear

Received 23 June 2010
* Supported by Natural Science Foundation of Hebei Province (A2008000421)
1) E-mail: whmw@sina.com.cn

gluon radiative processes and non-linear gluon recombination effects are included.

For experimental information about neutrons is unavailable, the net-baryon yield has to be estimated from the net-proton yield. The conversion from the net-protons, $N_{\rm p}$, to the net-baryons, $N_{\rm B}$, can be given as $N_{\rm B}=(2\pm0.1)N_{\rm p}$ at mid-rapidity and $N_{\rm B}=(2.1\pm0.1)N_{\rm p}$ at forward rapidities [11]. The experimental data for net proton production at the nucleon-nucleon center of mass energy, $\sqrt{s_{\rm NN}}=62.4$, 200 GeV are given in Refs. [11] and [12], respectively. By a χ^2 analysis of the experiment data, the normalization constant C, which is introduced for the lack of knowledge on the hadronization process [13, 14], can be extracted at different $\sqrt{s_{\rm NN}}$. If we assume that the constant C has an exponent dependence of $\sqrt{s_{\rm NN}}$ [15], the normalization constant at LHC energies could be calculated and the predicted results for the net-proton $p_{\rm T}$ spectra could also be given at LHC energies of $\sqrt{s_{\rm NN}}=2.76$, 3.94, and 5.52 TeV. In the following, the saturation scale of the nucleus is given by fixing to HERA data [16], and the valence fragmentation functions are given by the Albino-Kniehl-Kramer (AKK08) [17] parameterizations. Here, as in Ref. [14], the medium-modified effect for the fragmentation functions is not considered for $p_{\rm T}<3$ GeV [18, 19].

2 Method

By including the fragmentation function of a quark into net protons, the cross section for the production of a net-proton in nucleus-nucleus (A+A) collisions can be given by [4, 7]

$$\frac{{\rm d}N}{{\rm d}^2\vec{p}_{\rm T}{\rm d}y} = K\frac{C}{(2\pi)^2}\int_{x_{\rm F}}^1\frac{{\rm d}z}{z^2}D(z,Q^2)x_1q_v(x_1,Q^2)\varphi(x_2,q_{\rm T}), \quad (1)$$

where $p_{\rm T}$ is the hadron transverse momentum, z is the fraction of the quark energy carried by the baryon fragment, K=1.6 is a next-to-leading (NLO) order QCD correction [20]. $q_{\rm T}=\sqrt{p_{\rm T}^2+m^2}/z$ is the quark momentum with the nucleon mass $m=0.938$ GeV, $x_{\rm F}=\sqrt{p_{\rm T}^2+m^2}/\sqrt{s}\,\exp(y)$ is the Feynman-x, and $x_1=q_{\rm T}/\sqrt{s}\,\exp(y)$, $x_2=q_{\rm T}/\sqrt{s}\,\exp(-y)$. $D(z,Q^2)$ is the fragmentation function of a quark into net protons with $Q^2=p_{\rm T}^2+m^2$. The valence quark distribution of a nucleus $q_{\rm v}=N_{\rm part}q_{\rm v,N}$, where $q_{\rm v,N}$ is the valence quark distributions of individual nucleons, and the estimated numbers of participants $N_{\rm part}$= 315, 357, and 359 for $\sqrt{s_{\rm NN}}$=62.4, 200, and 5520 GeV [11, 21].

In Eq. (1), the nuclear unintegrated gluon distribution can be obtained from the forward dipole scattering amplitude, $N(x,r_{\rm T})$, through the Fourier transform [7]

$$\varphi(x,q_{\rm T}) = \int{\rm d}^2\vec{r}_{\rm T}{\rm e}^{{\rm i}\vec{q}_{\rm T}\cdot\vec{r}_{\rm T}}N(x,r_{\rm T}) = 2\pi\int_0^\infty r_{\rm T}{\rm d}r_{\rm T}N(x,r_{\rm T})J_0(r_{\rm T}q_{\rm T}), \quad (2)$$

where $r_{\rm T}$ is the quark dipole transverse size, and J_0 is the zeroth-order Bessel function of the first kind. In order to describe the fact that the gluon density is small at $x\to1$, a factor $(1-x)^4$ should also be multiplied in Eq. (2). The dipole scattering amplitude on a nucleus should be determined from the nonlinear evolution equation [10, 22]. However, since an exact solution of the nonlinear evolution is very difficult, a simple Glauber-like formula is used [4],

$$N(x,r_{\rm T})=1-\exp\left\{-\frac{1}{4}[r_{\rm T}^2Q_{\rm s}^2(x)]^{\gamma(x,r_{\rm T})}\right\}, \quad (3)$$

where the saturation scale of the nucleus can be given as [23]

$$Q_{\rm s}^2(x)=Q_0^2A^{1/3}(x_0/x)^\lambda.$$

For heavy $A\sim200$ targets, we use $Q_0^2=0.3$ GeV^2 as Ref. [23]. Parameters $x_0=0.0003$, and $\lambda\approx0.3$ are fixed to HERA data [16]. $\gamma(x,r_{\rm T})$ denotes the anomalous dimension of the gluon distribution. In the classical Golec-Biernat and Wusthoff (GBW) model [16], the anomalous dimension $\gamma=1$ and the Fourier transform of $N(x,r_{\rm T})$ can be performed analytically,

$$\varphi(x,q_{\rm T})=\frac{4\pi}{Q_{\rm s}^2(x)}\exp\left(-\frac{q_{\rm T}^2}{Q_{\rm s}^2(x)}\right). \quad (4)$$

In what follows, two distinct phenomenological models constructed to describe the RHIC data in d+Au collisions are considered. One is the DHJ model [7], in which

$$\gamma(x,r_{\rm T})=\gamma_{\rm s}+(1-\gamma_{\rm s})\frac{\lg[Q^2/Q_{\rm s}^2(x)]}{\lambda y+{\rm d}\sqrt{y}+\lg[Q^2/Q_{\rm s}^2(x)]}, \quad (5)$$

with $y=\lg(1/x)$, $d=1.2$ and $\gamma_{\rm s}=0.628$. $Q^2=1/r_{\rm T}^2$ is the inverse transverse size of the dipole, and $r_{\rm T}$ is replaced by $r_{\rm T}\approx1/q_{\rm T}$ to make the Fourier transform tractable. The other is the BUW model [8],

$$\gamma(x,r_{\rm T})=\gamma_{\rm s}+(1-\gamma_{\rm s})\frac{(\omega^a-1)}{(\omega^a-1)+b}, \quad (6)$$

where $\omega=1/(r_{\rm T}Q_{\rm s}(x))$ and the two free parameters $a=2.82$ and $b=168$ are fitted to the RHIC data on hadron production in d+Au collisions. In Fig. 1, we plot the quark momentum dependence of γ at x=0.1 (solid curves), 0.01 (dashed curves), and 0.001 (dotted curves) for the DHJ and BUW models. It is shown

that there is a stronger $q_{\rm T}$ dependence with the BUW model than that with the DHJ model at the same x.

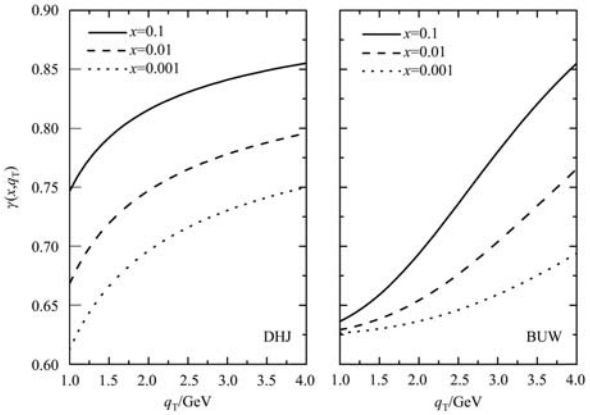

Fig. 1. The anomalous dimension γ versus $q_{\rm T}$ at x=0.1 (solid), 0.01 (dashed) and 0.001 (dotted) for the DHJ (left) and BUW (right) models.

In order to extract the normalization constant C from the experimental data, we recall the χ^2 method [24],

$$\chi^2=\sum_i \frac{\left(\dfrac{{\rm d}N}{{\rm d}^2p_{\rm T}{\rm d}y}|^{\rm data}_{y,j}-\dfrac{{\rm d}N}{{\rm d}^2p_{\rm T}{\rm d}y}|^{\rm theo}_{y,j}\right)^2}{\left(\dfrac{{\rm d}N}{{\rm d}^2p_{\rm T}{\rm d}y}|^{\rm err}_{y,j}\right)^2}, \quad (7)$$

where $\dfrac{{\rm d}N}{{\rm d}^2p_{\rm T}{\rm d}y}|^{\rm theo}_{y,j}$ is the theoretical values calculated by Eq.(1) at selected rapidities.

$$\frac{{\rm d}N}{{\rm d}^2p_{\rm T}{\rm d}y}|^{\rm data}_{y,j} \quad \text{and} \quad \frac{{\rm d}N}{{\rm d}^2p_{\rm T}{\rm d}y}|^{\rm err}_{y,j}$$

indicate the corresponding experimental data and systematic errors in the experiments at RHIC [11, 12].

3 Results and discussion

In this work, Eqs. (1) and (2) are used to calculate the theoretical results,

$$\frac{{\rm d}N}{{\rm d}^2p_{\rm T}{\rm d}y}|^{\rm theo}_{y,j}.$$

As shown in Eq. (2), where the Bessel function oscillates rapidly, it is difficult to perform the Fourier transform numerically. In our calculation, by means of the Bessel function simulated by a polynomial for $r_{\rm T}q_{\rm T}<8$ and a polynomial with the sine (cosine) function for $r_{\rm T}q_{\rm T}\geqslant 8$, the oscillating integration is solved by the Simpson method. In Eq. (1), employing isospin symmetry of the proton and neutron, we use the CTEQ6 distribution functions for the valence quark distribution in the proton and neutron [25], and the AKK08 fragmentation functions for the valence quark to net-protons, where the baryon number conservation is reconsidered as Ref. [14]. By a χ^2 analysis of the experimental data given by BRHAMS [11, 12], it is found that the value of the normalization constant C=1.02 (0.89) and 0.46 (0.44) at $\sqrt{s_{\rm NN}}$ = 62.4 and 200 GeV with the DHJ (BUW) model.

The theoretical results for the net-proton transverse momentum spectra at 62.4 and 200 GeV are shown in Figs. 2 and 3, respectively. The curves are the theoretical results for the DHJ (solid), BUW (dashed), and classical GBW (dotted) models. The experimental data come from BRHAMS [11, 12]. Since the anomalous dimension γ has a stronger $q_{\rm T}$ dependence for the BUW model than that for the DHJ model, as shown in Figs. 2 and 3, a little steeper trend can be seen for the results with the BUW model than that with the DHJ model. It is also shown that both results are in good agreement with the experimental data.

In order to give a prediction of the results in Pb+Pb collisions at LHC energies, we assume [15]

$$\frac{C_1N_{\rm part1}}{C_2N_{\rm part2}}=\left(\frac{\sqrt{s_{\rm NN2}}}{\sqrt{s_{\rm NN1}}}\right)^{\alpha}, \quad (8)$$

where α =0.57 (0.49) for DHJ (BUW) model through using the parameters C extracted from BRAHMS. In Fig. 4, by means of the DHJ model, the net-proton transverse momentum spectra are shown for

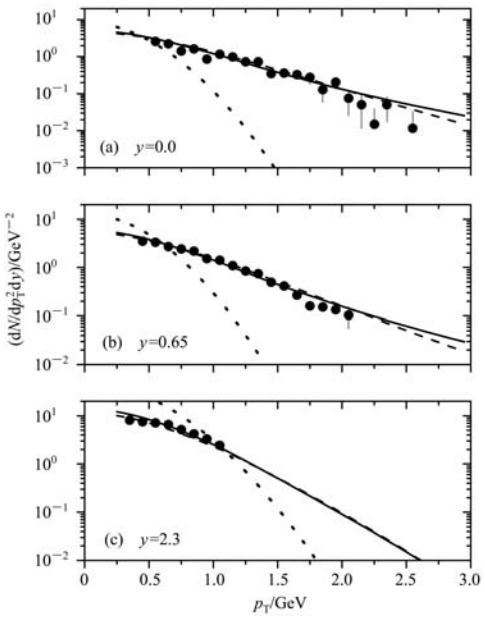

Fig. 2. Net-proton transverse momentum spectra for Au+Au collisions at $\sqrt{s_{\rm NN}}$ = 62.4 GeV for $y\sim 0$ (a), $y\sim 0.65$ (b) and $y\sim 2.3$ (c). The curves are the results for the DHJ (solid), BUW (dashed), and GBW (dotted) models. The experimental data are taken from BRAHMS.

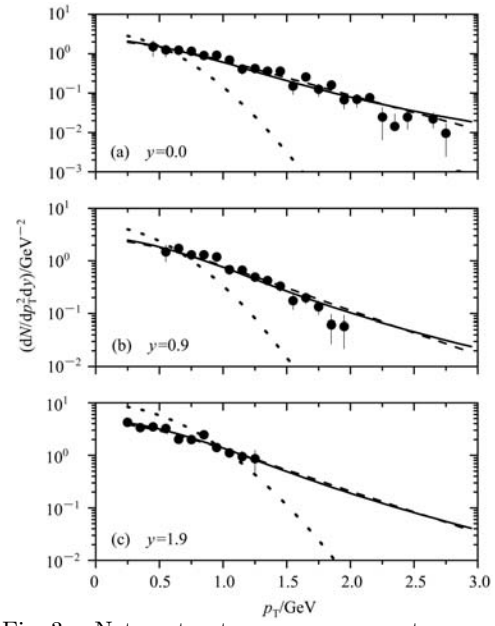

Fig. 3. Net-proton transverse momentum spectra for Au+Au collisions at $\sqrt{s_{\rm NN}} = 200$ GeV for $y \sim 0$ (a), $y \sim 0.9$ (b) and $y \sim 1.9$ (c). The figure captions are the same as Fig. 2.

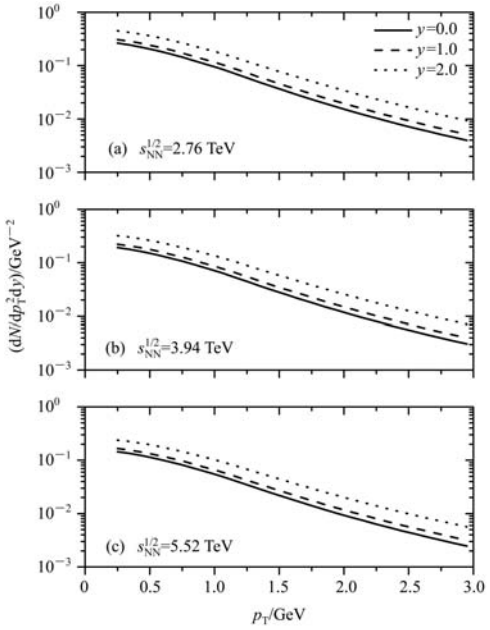

Fig. 4. Net-proton transverse momentum spectra for Pb+Pb collisions at LHC energies of $\sqrt{s_{\rm NN}}$ = 2.76, 3.94, 5.52 TeV (from up to down). The curves are the results for $y \sim 0$ (solid), $y \sim 1$ (dashed) and $y \sim 2$ (dotted).

$\sqrt{s_{\rm NN}}$ = 2.76 (a), 3.94 (b) and 5.52 (c) TeV [26]. The curves are the results at selected rapidities, y=0 (solid), 1 (dashed) and 2 (dotted), and the theoretical results will be examined by the forthcoming experimental data.

In summary, by means of the DHJ and BUW models, the net-proton transverse spectra are studied with the AKK08 fragmentation parametrization, where the medium-modified effect is not considered as in Ref. [14]. It is shown that the theoretical results are in good agreement with the experimental data from BRAHMS. Then, by assuming the constant C should have an exponent dependence of $\sqrt{s_{\rm NN}}$, the predicted results at LHC energies are also given with the DHJ model. In this paper, for the valence quark momentum fraction $x_1 > 1$ at large rapidity, which is out of the effective range of CTEQ6, only the results for $|y| < 2.3$ are given. With a further investigation, the theoretical results at large rapidity will be given in the near future.

References

1 Gelis F, Iancu E, Jalilian-Marian J et al. hep-ph/1002.0333
2 Iancu E, Itakura K, Munier S. Phys. Lett. B, 2004, **590**: 199
3 Arsene I, Bearden I G, Beavis D et al. Phys. Rev. Lett., 2004, **93**: 242303
4 Kharzeev D, Kovchegov Y V, Tuchin K. Phys. Lett. B, 2004, **599**: 23
5 Baier R, Mehtar-Tani Y, Schiff D. Nucl. Phys. A, 2006, **764**: 515
6 Albacete J L, Marquet C. Phys. Lett. B, 2010, **687**: 174
7 Dumitru A, Hayashigaki A, Jalilian-Marian J. Nucl. Phys. A, 2006, **770**: 57
8 Boer D, Utermann A, Wessels E. Phys. Rev. D, 2008, **77**: 054014
9 Balitsky I. Nucl. Phys. B, 1996, **463**: 99
10 Kovchegov Y V. Phys. Rev. D, 1999, **60**: 034008
11 Arsene I C, Bearden I G, Beavis D et al. Phys. Lett. B, 2009, **677**: 267
12 Bearden I G, Beavis D, Besliu C et al. Phys. Rev. Lett., 2004, **93**: 102301
13 Albacete J L. Phys. Rev. Lett., 2007, **99**: 262301
14 Mehtar-Tani Y, Wolschin G. Phys. Rev. C, 2009, **80**: 054905
15 Mehtar-Tani Y, Wolschin G. Phys. Lett. B, 2010, **688**: 174
16 Golec-Biernat K, Wusthoff M. Phys. Rev. D, 1999, **59**: 014017
17 Albino S, Kniehl B A, Kramer G. Nucl. Phys. B, 2008, **803**: 42
18 Armesto N, Cunqueiro L, Salgado C A et al. JHEP, 2008, **0802**: 048
19 Fries R J, Muller B, Nonaka C et al. Phys. Rev. Lett., 2003, **90**: 202303
20 Dumitru A, Hayashigaki A, Jalilian-Marian J. Nucl. Phys. A, 2006, **765**: 464
21 Kuiper R, Wolschin G. Ann. Phys., 2007, **16**: 67
22 Kovchegov Y V. Phys. Rev. D, 2000, **61**: 074018
23 Kharzeev D, Levin E, Nardi M. Nucl.Phys. A, 2004, **730**: 448
24 WANG H M, SUN X J, HOU Z Y. HEP & NP, 2007, **31**(11): 1040 (in Chinese)
25 Kretzer S, LAI H L, Olness F et al. Phys. Rev. D, 2004, **69**: 114005
26 Aamodt K, Abel N, Abeysekara U et al. Eur. Phys. J. C, 2010, **65**: 111